APPLICATION OF HYPERSPECTRAL IMAGE DATA FOR SPECIES DETECTION AND BIOMASS ESTIMATION OF SUBMERGED MACROPHYTES IN UK CHALK STREAMS

F. Visser [a, *] and R.A. Hill [b]

[a] Institute of Science and the Environment, University of Worcester, Henwick Grove, Worcester, WR2 6AJ, UK - f.visser@worc.ac.uk

[b] Bournemouth University, Talbot Campus, Fern Barrow, Poole, Dorset, BH12 5BB, UK - rhill@bmth.ac.uk

KEYWORDS: hyperspectral remote sensing, submerged macrophytes, chalk streams, PSF, image deconvolution

ABSTRACT:

Expected improvements of spatial and spectral resolution of remote sensing data in the near future will finally enable their application for the monitoring of some of the UK's most biodiverse ecosystems: lowland chalk streams. The possibility to remotely map cover extent and submergence depth of chalk stream macrophytes could improve biomass estimates and help understanding of macrophyte community dynamics. This study aims to improve *Ranunculus* (Water crowfoot) submergence depth estimates from a Specim Eagle hyperpsectral image taken of the River Frome in Dorset, UK by combining data from previous studies. NDVI values calculated from *Ranunculus* vegetation spectra measured with a GER1500 show a depth dependence, which corresponds well with modelled values. NDVI values extracted from the image data do not show a similar relationship. The results highlight the difficulty of obtaining accurate submergence depth information when vegetation cover and submergence depth vary at sub-pixel level.
Data quality issues also hamper image analysis at this level of detail. Blurring/smearing of the data will have affected the NDVI-submergence depth relationship derived from the image. An attempt was made to improve the data quality by estimating an empirical Point Spread Function (PSF) from the bank vegetation - river water interface and trialling different deconvolution algorithms and input parameters. The application of this method was unsuccessful and specified some of the limitations of a technique that has been successfully applied in other situations.

1. INTRODUCTION

1.1 Chalk streams and *Ranunculus* communities

Groundwater fed 'chalk streams' form a unique and important habitat in a national and international context. They are found in parts of the United Kingdom underlain by chalk bedrock, which determines their stable flow conditions, chemical water quality and high water clarity. In many chalk streams vegetation is dominated by river water crowfoot (*Ranunculus penicillatus var pseudofluitans*). This macrophyte forms a key component in the structural and biological diversity of the streams, by providing food and shelter for macroinvertebrates, shellfish and fish. *Ranunculus* community growth tends to be variable and may be influenced by stress factors such as water abstraction and mute swan grazing. The true dynamics are however not well understood, partly because of the difficulty of field data collection. There is no standardised method to sample macrophytes and methods used are often destructive and labour-intensive (Porteus et al., 2011). Due to their physical characteristics (e.g. low sediment concentration and shallow depth) chalk streams could make good candidates to apply remote sensing techniques as an alternative, non-destructive *Ranunculus* monitoring method.

1.2 Study aims

Some studies have started looking at using remote sensing for submerged chalk stream macrophyte species detection and biomass estimation, but so far they are few in number. Visser and Smolar-Žvanut (2009) investigated detectability of various species from above the water surface in the river Wylye in Wiltshire, using a GER1500 field spectroradiometer. Work by Hill at al. (2009) on the River Frome in Dorset, looked at estimating *Ranunculus* submergence depth from a Specim Eagle hyperspectral image. Their aim was to map abundance of *Ranunculus* and identify grazing pressure from mute swans.
The study described in this paper firstly combines data from both these previous studies with the aim to improve abundance mapping/biomass estimation. The detailed vegetation spectra obtained in the field by Visser and Smolar-Žvanut are used to obtain more accurate submergence depth estimates from the hyperspectral image data of Hill et al. However, during the course of the study it became clear that quality issues regarding the Eagle data hampered this first aim, therefore improvement of the data quality became a secondary aim of the study.

* Corresponding author. This is useful to know for communication with the appropriate person in cases with more than one author.

2. DATA AND METHODS

2.1 Field spectroradiometer observations

During the study by Visser and Smolar-Žvanut (2009) reflectance spectra were measured with a GER1500 above the water surface for a number of macrophyte species located at varying depths below the water surface. Spectra were also measured from vegetation specimens placed on a low reflectance black cloth out of the water. Based on the out-of-the-water vegetation spectra, submerged spectra were modelled for different depths, assuming attenuation of light by water absorption only (see Fig. 1). Reflectance from vegetation at depth l_{sim} were calculated for each wavelength by:

$$\frac{I_{sim}}{I_0} = 10^{-(A_s + \alpha_\lambda . l_{sim})} \quad (1)$$

Where I_0 is the incident intensity of the light, A_s is the absorbance calculated from the out-of-the-water reflectance measurements, α_λ is the absorption coefficient at wavelength λ (cm^{-1}), and l is the path length (cm).

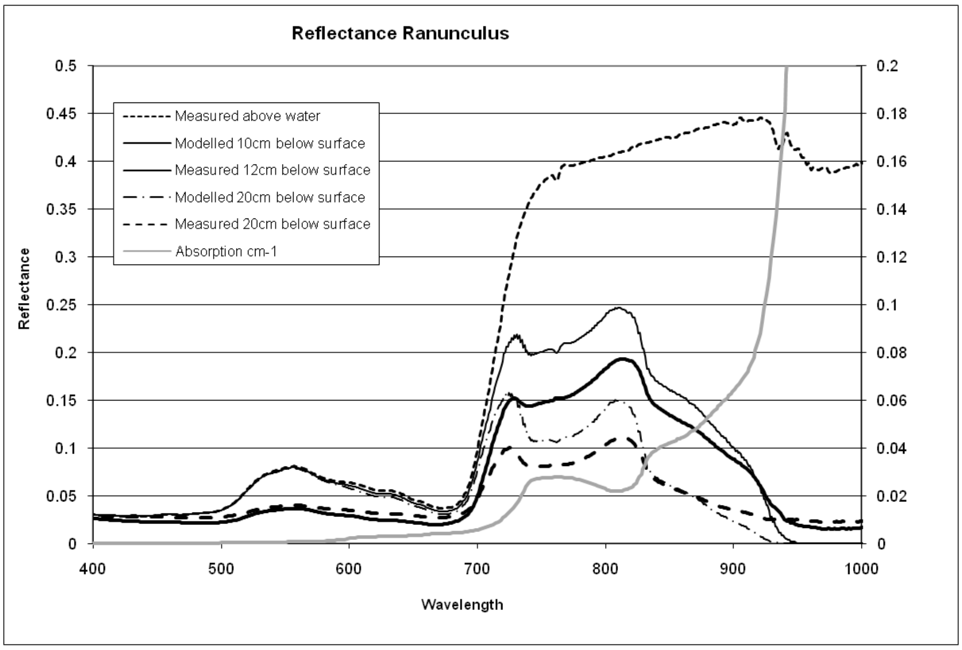

Figure 1. Measured and modelled reflectance spectra for *Ranunculus* above and at various depths below the water surface.

Shape-wise the measured spectra corresponded well with modelled spectra based. The height difference between measured and modelled curves, increasing at lower wavelength, is expected to result from ignoring backscatter. Especially reflectance in the NIR is strongly affected by water absorption, but for the relatively shallow submergence depth of many macrophytes, the shape of the NIR part of the spectrum can still help discriminating different species. The species specific effect of the absoroption with depth can also be used to estimate submergence depth and may be used to improve on the waveband rationing as done by Hill et al. (2009).

2.2 The Specim Eagle hyperspectral image and ground data collection

Hyperspectral image data of the River Frome was collected with a Specim AISA Eagle sensor on 24/06/2008 during a NERC ARSF flight. The data covers a 20 km stretch of the downstream part of River Frome in Dorset and consists of 126 bands between 470nm and 970nm with 1m ground resolution. During the flight ground data was collected by a team from Bournemouth University. Atmospheric data was not collected on site at the time of the flight.

Part of the ground data collected at the time of the flight are transects along which vegetation cover and submergence depth were recorded. Six transects were taken at each of two locations along the river near East Stoke. Each transect consists of 25x25cm quadrants for which total cover and average submergence depth were recorded. For this study pixel spectra were extracted from the image at the locations of the transect measurements. The image data spectra were then compared with the field spectoradiometer results to validate submergence depth – wavelength relationship derived from the field spectroradiometer data.

2.3 Image restoration

Initial assessment of the hyperspectral image data immediately brought up data quality issues. A blurring/smearing was observed, which was especially clear at the boundary between river and vegetated bank. In the studied reach the transition between bank and water generally is less than a meter wide and mixing of the bank and water signals should not exceed two pixels. Initially the blurring effect was attributed to a combination of instrumental, atmospheric and environmental scattering, i.e. 'adjacency effects'. Due to lack of atmospheric data for the collection date, an alternative method was attempted to reduce the blurring effect. This approach consisted of the estimation of an empirical Point Spread Function (PSF) and deconvolution of the data with this function. Several recent publications present the results of deconvolution alogrithms, often with some success (e.g. Jackett et al., 2011; Kopeika et al., 2003; Rahmani et al, 2008; Ruiz and López, 2002). In many cases a-priori information is available on the shape of the PSF, however some studies have derived it from local contrast in image data values (e.g. Ruiz and López, 2002).

A degraded image can be described as follows:

$$L_m(x_0, y_0) = \sum_{ij} PSF\ (i - x_o, j - y_o) \cdot L_T(i, j) \qquad (2)$$

Where L_m (x_0, y_0) is the measured radiance from pixel (x_0, y_0), PSF the point spread function and L_T (i,j) the true radiance of pixel (i,j). For this study the PSF was empirically estimated using a method similar to that proposed by Ruiz and López (2002). Their restoration approach for SPOT images makes use of a PSF, which is estimated by extracting a Linear Spread Function (LSF) perpendicular to the edge of dam structures in ponds in the image. The derivative of the LSF with respect to position is the Point PSF. For the current study 5 radiometric profiles are plotted perpendicular the river bank. A function is fitted through the combined data points and a first derivative is estimated from the smooth radiometric step. Next a 2-dimensional PSF is obtained by assuming a uniform step in all directions and rotating and averaging the LSF across a 11x11 sized filter, which is then normalized. Deconvolution is performed with the MATLAB Image Processing Toolbox (Gonzalez et al., 2004), using both the Wiener and Lucy Richardson deconvolution tools. The Wiener deconvolution makes use of a NOISEPOWER (NSPR) which is estimated as MN[σ^2_η + m^2_η] where M and N are the dimensions of the processed image and the noise variance and noise squared mean. Finding the optimal value for this parameter however requires experimenting (Gonzalez et al., 2004). Subsequent information about the data showed that the blurring was largely the result of a sensor issue, for which so far no satisfactory solution is available (Panousis, 2010). The deconvolution results will be discussed in the light of this sensor information.

3. RESULTS

3.1 Field spectroradiometer vs. modelled vs. image data reflectance spectra

For initial comparison of the *Ranunculus* spectra from the three data sources NDVIs were caclulated using the 675nm red band and the 798nm NIR band. These wavelenghts were expected to be least affected by atmosphteric conditions, while showing a differential response to water absostion. The NDVI calcuated from the field spectroradiometer spectra, modeled spectra and the image derived spectra will be referred to as $NDVI_{field}$ $NDVI_{model}$, $NDVI_{image}$, respectively.

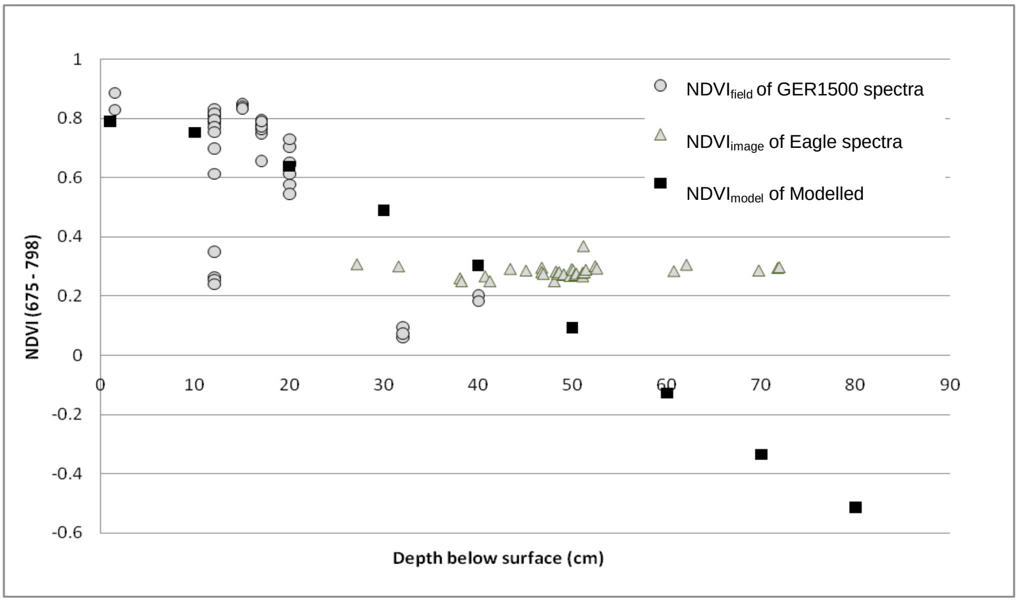

Figure 2. NDVI – submergence depth scatterplots for measure, modelled and image spectra.

Fig. 2 shows the NDVI calculated from each data source plotted against submergence depth. $NDVI_{model}$ and $NDVI_{field}$ correspond well as was expected from previous comparison of the spectra. Most outliers with relatively low NDVI at 12cm and 32cm depth were noted to have microalgae cover on the macrophyte leaves. $NDVI_{image}$ corresponded less well with the others. Due to the blurring of the radiometric data individual quadrant depth values were expected to be of little use. The values plotted in Fig. 2 were therefore obtained by averaging adjacent quadrants of all 6 transects at both sites and the two resulting depth transects were smoothed using a moving average. The averaging reduced the depth data range, but did not clearly improve the correlation. For most of the measured quadrants the vegetation cover was 100%, though quadrants near the edges of *Ranunculus* patches contained less vegetation cover.

The non-vegetated parts of these quadrants will affect the average radiance spectrum measured within the quadrant, though their number (app. 35% of vegetated pixels) should not have affected NDVI correlation with depth to the current extent. There may have been variation in submergence depth within quadrants, which will also affected the correlation, but the blurring/smearing of the pixel radiance values is expected to have had most influence on the NDVI – submergence depth correlation.

3.2 Empirical PSF estimation

Figure 3a shows radiometric profiles extracted from the Eagle image at five locations perpendicular to the river bank (Fig. 3b). Data was extracted for three bands (34, 53 and 77). Wavelength did not seem to clearly determine the shape of the smooth radiometric step.

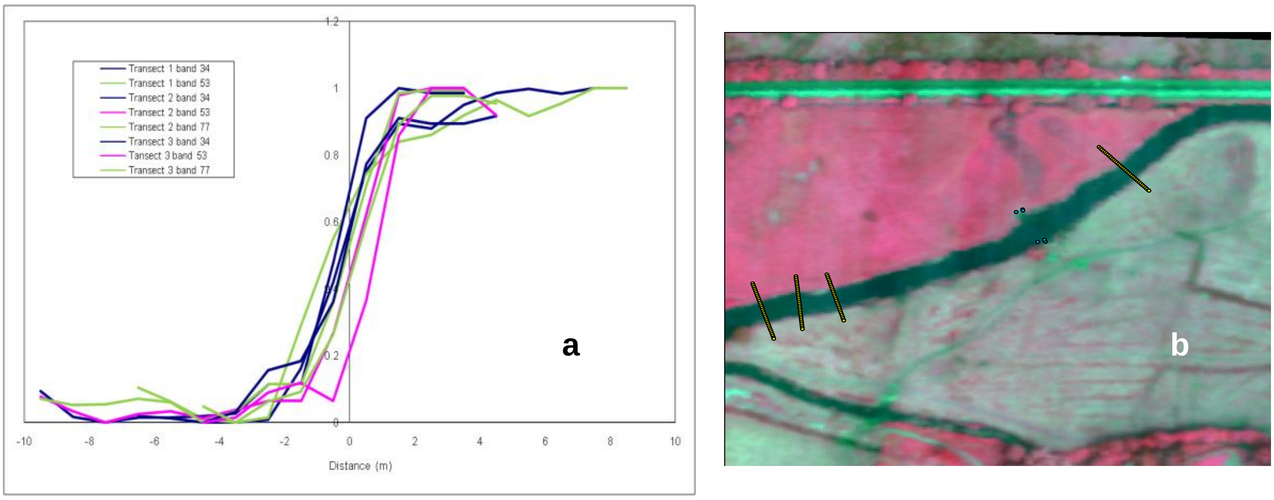

Figure 3. Radiometric profiles (a) extracted from three bands of the Eagle image (b) at five locations perpendicular to the river bank.

A Gaussian function was fitted through the extracted data points and the first derivative LSF derived from this is shown in Fig. 4a. The 2D PSF filters derived from the LSF are shown in Fig. 4b (11x11m) and 4c (5x5m).

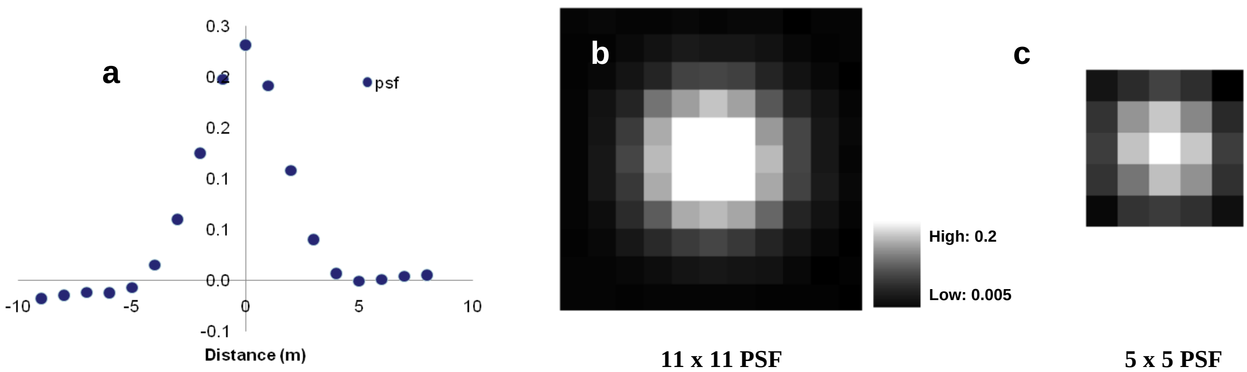

Figure 4. LSF obtained from radiometric profile (a), 2D PSF derived from LSF with 11x11m (b) and with 5x5m (c) dimension.

3.3 Deconvolution filter results

The Wiener and Lucy-Richardson deconvolution algorithms were executed with both PSF filters sizes. The Wiener algorithm was also used with a range of NSPR values. The results of the deconvolution were assessed visually from the resulting images, and in more detail, by re-extracting and plotting the radiometric profiles that were used for PSF creation.

Generally the Lucy-Richardson deconvolution seemed to produce best results, but none of the tested input parameter configurations produced a convincing image improvement. Fig. 5 shows the radiometric profiles taken from both the Lucy-Richardson and Wiener deconvolution image results. Profiles from the Lucy-Richardson image results are shown for both PSF filter sizes. Wiener deconvolution results are only shown for the 5x5m filter using an optimal NSPR parameter value (0.1). The Wiener deconvolution did not steepen the profile at all. Both Lucy-Richardson trails do show improvements for steepness, but in each case noise/variation beyond the step seem to increase as well compared the original data, which reduces the benefit of the deconvolution.

The optimal NSPR value for the Wiener deconvolution was estimated by trying a range of parameter values. Fig. 6a shows the results for a number of these trials which made use of the 11x11 PSF filter. Again little improvement of image sharpness is achieved with any of the parameter settings, but a too high NSPR value (1) clearly results in too much smoothing of the data. A too low value (0.01) on the one hand seems to steepen the profile, but also produces a 'ringing' parallel to the radiometric step, which is visible in the resulting image as ridges along each of the river banks (Fig. 6b).

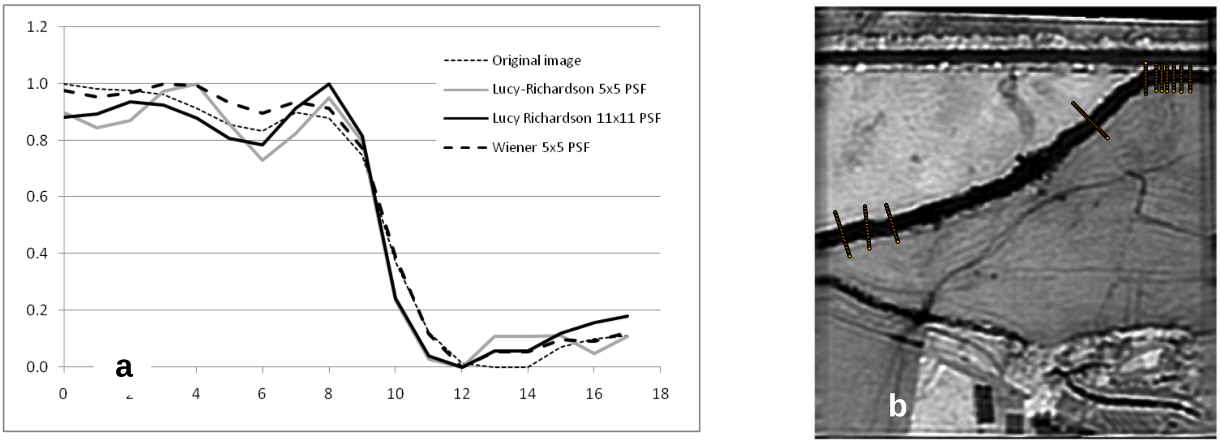

Figure 5. Radiometric profiles of results of 3 deconvolution methods (a) and image results of Lucy-Richardson deconvolution for band 77 (b)

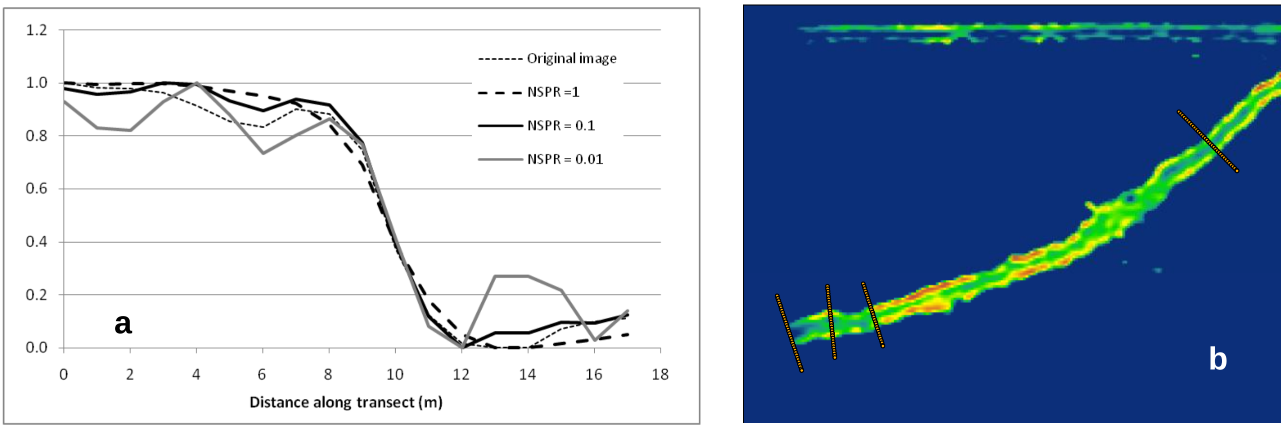

Figure 6. Radiometric profiles of results for Wiener deconvolution with NSPR 1, 0.1 and 0.01 (a) and an example of 'ringing' in the data when NSPR values become too low (here 0.01), as shown for band 77 by ridges on the river bed, parallel to the river bank (b)

4. DISCUSSION

4.1 Field data comparison

$NDVI_{field}$ values calculated from field spectroscopy measurements of submerged *Ranunculus* vegetation show some correlation with submergence depth (Fig. 2) as was observed by Hill et al. (2009) for the Specim Eagle data. The $NDVI_{modeled}$ – submergence depth correlation, based on out-of-the-water *Ranunculus* spectra using water absorption only, corresponds with the $NDVI_{field}$ – submergence depth correlation. The $NDVI_{image}$ values extracted from the Specim Eagle image however do not correlate with depth in the same way. Variation of $NDVI_{image}$ values with depth is limited to a much smaller range. There are a number of possible explanations for this. Firstly the Eagle data has not yet been atmospherically corrected. Although the effect was not expected to be very big for the chosen wavelengths and normalized radiance values, the 675nm values would have been affected more strongly resulting in overestimation of the NDVI values. Secondly sub-pixel variation in vegetation cover and depth will affect reliability of the data to some extent. Finally the blurring of the image data is expected to have had a considerable impact through averaging-out the higher and lower NDVI values.

The field spectroradiometer results look promising for remote detection of *Ranunculus* submergence depth, which could lead to vegetation biomass estimates. The airborne imaging spectroscopy data used in this study was however not well suited for applications at the level of detail required for chalk stream studies. Although improvements can be made through atmospheric correction of the data and resolution of the sensor problems, ultimately applications remain limited to areas with large vegetation patches and relatively uniform vegetation depth. The combination of strong depth dependence of the NIR vegetation signal and variation in submergence depth and vegetation cover at sub-pixel level make it difficult to obtain vegetation biomass estimates with the current resolution of the hyperspectral imagery. With the development of higher spatial resolution sensors, or perhaps through fusion with hyperspatial data of lower spectral resolution, better results are likely to be achieved in the near future. Combination with of object-based image analysis techniques can also help identify boundaries of vegetation patches more accurately.

4.2 Image restoration

Data quality of the Specim Eagle image has been likely to affect the NDVI – submergence depth correlations discussed above. An attempt to restore the data with an empirical Point Spread Function (PSF) did not resolve the blurring/smearing problem. The Lucy-Richardson deconvolution algorithm showed best results, but the advantage of a slight increase in the steepness of the radiometric profile was offset by undesirable enhancement of variation elsewhere in the image (e.g. 'ringing' along edges in the image).

A number of different reasons can be identified to explain the disappointing results:
1) The empirical PSF estimate is likely to be a major reason; more accurate estimates may improve deconvolution results, though heterogeneity of the bank and water signal and presence of submerged vegetation in the optically shallow water may limit further improvements.
2) A recent report ascribe the blurring in the Eagle data to light falling onto a frame-transfer CCD during the shifting of image data into a temporary storage buffer. This stray light is registered as a smear in each line (Panousis, 2010). So, error found in the data may not be adjacency related (though a considerable range was also noted in along track bank/river boundaries) and the empirical PSF is only valid in the along-track direction, while the same line-spread function was used to create the PSF in all directions.
3) Trials of deconvolution with a range of different input parameters indicated additional factors that significantly influenced the deconvolution outcomes:
   - The different deconvolution algorithms (Wiener and Lucy Richardson) generated different results.
   - The NOISEPOWER (NSPR) input parameter in the Wiener method strongly influenced the restoration outcome.
   - The choice of PSF dimensions is arbitrary but affects results by smoothing data or enhancing noise.
4) Noise in the image is likely to be too high to allow image restoration as already suggested by Rahmani et al. (2008) and Kopeika et al. (2003). If too much noise is present this will be amplified and can actually reduce image quality. In other studies some of the issue were resolved by either starting with a denoising filter (Rahmani et al., 2008) or by using alternative deconvolution methods which improved results (Kopeika et al., 2003; Jackett et al., 2011). None of these alternative methods have been attempted here.

The above discussion shows that there is room to improve the image restoration procedure, but also that the, to some extent arbitrary, parameter input compromises the suitability of the approach for studies where a similar level of detail is required

REFERENCES

Gonzalez, R.C., Woods, R.E., Eddins, S.L., 2004. Digital *Image Processing Using MATLAB*. Pearson Ed. p. 609.

Hill, R.A., O'Hare, M.T., Stillman, R.A. and Gozlan, R.E., 2009. Hyperspectral remote sensing of river macrophyte vegetation: towards an assessment of wildfowl and fish habitat quality. In: *RSPSoc Annual Conference: New Dimensions in Earth Observation*, 8-11 September 2009, Leicester.

Jackett, C.J., Turner, P.J., Lovell, J.L., Williams, R.N., 2011. Deconvolution of MODIS imagery using multiscale maximum entropy. *Remote Sensing Letters* 2(3), pp. 179-187.

Kopeika, N.S., Rotman, S.R., Taig, I., 2003. Effects of image restoration on target acquisition. *Optical Engineering* 42(2), pp. 534-540.

Panousis, I, 2010. Light (smear) carried from the unrecorded Eagle bands on the infra-red end. On-line document: http://arsf-dan.nerc.ac.uk/trac/raw-attachment/ticket/357/EagleUnrecordedSmear-2.pdf [accessed 31/04/2011].

Rahmani, P., Vozel, B., Chehdi, K., 2008. Sequential blind PSF estimation and restoration of aerial multispectral images. *Lecture notes in computer science* 5259, pp. 410-421.

Ruiz, C.P. and López, F.J.A., 2002. Restoring SPOT images using PSF-derived deconvolution filters. International *Journal of Remote Sensing* 23(12), pp. 2379-2391.

Visser, F. and Smolar-Žvanut, N., 2009. Detecting Submerged Macrophytes in a UK Chalk Stream Using Field Spectroscopy. In: *RSPSoc Annual Conference: New Dimensions in Earth Observation*, 8-11 September 2009, Leicester, pp. 541-547.

Porteus, T.A., Short, M.J., Reynolds, J.C., Stubbing, D.N., Richardson, S.M. Aebischer, N.J., 2011. The impact of grazing by mute swans (Cygnus olor) on the biomass of chalkstream macrophytes. Game & Wildlife Conservation Trust On-line report. http://www.riverfrome.com/wp-content/uploads/2011/02/Impact-of-swan-grazing.pdf [accessed 31/04/2011].

ACKNOWLEDGEMENTS

The field spectroradiometer was on loan from the NERC Field Spectrometry Facility (FSF). The airborne remotely sensed data were collected under NERC ARSF award GB08-18. Additional funds for field work were provided by the University of Worcester and the Earth and Space Foundation.